Phys. Status Solidi RRL **7**, No. 11, 946–949 (2013) / **DOI** 10.1002/pssr.201308115

Passivation of aluminium–n$^+$ silicon contacts for solar cells by ultrathin Al_2O_3 and SiO_2 dielectric layers

James Bullock*, **Di Yan, and Andrés Cuevas**

Research School of Engineering, The Australian National University, Canberra, ACT 0200, Australia

Received 8 August 2013, revised 23 August 2013, accepted 23 August 2013
Published online 29 August 2013

Keywords silicon, solar cells, surface passivation, contact resistance, metal–insulator–semiconductor structures

* Corresponding author: e-mail james.bullock@anu.edu.au, Phone: +61 261 251 763

Ultra-thin thermally grown SiO_2 and atomic-layer-deposited (ALD) Al_2O_3 films are trialled as passivating dielectrics for metal–insulator–semiconductor (MIS) type contacts on top of phosphorus diffused regions applicable to high efficiency silicon solar cells. An investigation of the optimum insulator thickness in terms of contact recombination factor J_{0_cont} and contact resistivity ρ_c is undertaken on 85 Ω/□ and 103 Ω/□ diffusions. An optimum ALD Al_2O_3 thickness of ~22 Å produces a J_{0_cont} of ~300 fAcm^{-2} whilst maintaining a ρ_c lower than 1 mΩ cm^2 for the 103 Ω/□ diffusion. This has the potential to improve the open-circuit voltage by a maximum 15 mV. The thermally grown SiO_2 fails to achieve equivalently low J_{0_cont} values but exhibits greater thermal stability, resulting in slight improvements in ρ_c when annealed for 10 minutes at 300 °C without significant changes in J_{0_cont}. The after-anneal J_{0_cont} reaches ~600 fAcm^{-2} with a ρ_c of ~2.5 mΩ cm^2 for the 85 Ω/□ diffusion amounting to a maximum gain in open-circuit voltage of 6 mV.

1 Introduction The metal–silicon interface, required to contact diffused junction silicon solar cells, is known to host a large density of defects within the silicon band gap. These defects promote carrier recombination – an undesirable characteristic for this device. This issue is typically mitigated by employing deep dopant profiles that reduce the surface minority carrier concentration, which in this case is the limiting factor of surface recombination. However, at the same time, the high majority carrier concentration resultant from the dopant profile causes increased Auger recombination. Hence, the lowest achievable metal-contacted diffused region recombination factor J_{0_cont} is ~350 fAcm^{-2} for both phosphorus and boron diffusions, and slightly higher for aluminium alloyed p$^+$ regions [1]. To combat these large recombination factors, high efficiency solar cell architectures implement contact fractions of less than 5% and apply passivating dielectric films to the remainder of the surface. The non-contacted regions benefit from lighter diffusions, especially on the sunward side, introducing the need for a compromise between the two regions, contacted and passivated, in terms of dopant profile. This compromise is sometimes circumvented by applying the deep diffusions only locally under the contacts allowing the remainder of the surface to be lightly diffused. The fabrication of this architecture requires alignment of deep dopant diffusions and metallised regions, a complex process to be industrially implemented.

A possible improvement is to passivate the metallised surface regions with an ultra-thin dielectric, allowing a lighter (either local or global) dopant diffusion to be used. This dielectric must be sufficiently thin to present negligible resistance to current flow (possibly via quantum mechanical tunnelling) whilst being thick enough to provide appreciable surface passivation. The same ultra-thin layer can be applied to the entire wafer surface with a capping layer applied in the non-metallised regions [2–4].

The application of an ultra-thin dielectric under the contact, commonly referred to as a metal–insulator–semiconductor (MIS) type contact, has been implemented by research teams in the past. Green et al. used a thermally grown ~1.5 nm SiO_2 layer in their metal–insulator n$^+$p (MINP) type solar cells in the early 80's [5]. Later, Jäger-Hezel et al. [6] and Metz et al. [7] applied similar thermal oxide structures to their solar cells (a practice that has continued at ISFH [4]). More recently, the Angstrom level of control and excellent surface passivation afforded_ by atomic-layer-deposited (ALD) Al_2O_3 has been trialled as MIS contacts, both with oxygen plasma [2, 3] and water [8] as oxidising precursors. This Letter presents an investigation of the optimum dielectric thickness and potential benefit of applying MIS contacts to conventional diffused junction silicon solar cells. The recombination factor of the contacted phosphorus diffused region J_{0_cont} and the contact resistivity ρ_c are investigated as the two metrics of importance. Whilst a detailed solar cell simulation is required to analyse the effect of simultaneously altering J_{0_cont} and ρ_c, it can be taken as a general rule that ρ_c will not significantly contribute to the series resistance of most solar cells unless it exceeds ~1 mΩ cm². At this resistivity a high efficiency front-side metallisation scheme with a 5% fraction will produce a contact resistance R_c of ~40 mΩ cm² – accounting for ~5% of typical series resistance values.

Thermally grown SiO_2 and thermal ALD Al_2O_3 are trialled as potential dielectrics. Evaporated aluminium, recently shown to be compatible with industrial production [9], is used as the metal in all cases.

2 Experimental Symmetrical lifetime test structures were prepared using high resistivity 100 Ω cm, (100) oriented, float zone, p-type silicon wafers with a starting thickness of 500 ± 25 µm. The wafers were subjected to a 2 minute alkaline saw damage etch followed by surface polishing in a HF : HNO_3 solution. Following an RCA clean, the samples were diffused (~800 °C) using $POCl_3$ and driven-in (~950 °C) in a dedicated quartz furnace, producing a sheet resistance of ~50 ± 5 Ω/□. The resultant dopant profile was measured using an electrochemical capacitance–voltage profiler (WEP, CVP21) and is shown in Fig. 1. Dopant profiles were then etched back to one of the two points indicated in Fig. 1 using an alkaline etch. The resultant attributes of the two final dopant profiles are detailed in Table 1. At this point samples were coated (on both sides) with varying thicknesses of either ALD Al_2O_3 or thermal SiO_2. The Al_2O_3 was deposited at ~200 °C (Beneq TFS200 ALD) using trimethylaluminium and water as alternating precursors. Purge and pulse times were chosen to ensure a self-limiting reaction. No post-deposition anneal was performed on ALD Al_2O_3 coated samples prior to measurement. The thermal SiO_2 dielectrics were grown at 500 °C in O_2. All samples received an RCA clean and HF dip immediately prior to deposition or growth to ensure that native oxides were minimised. A thin (~10 nm) aluminium layer was evaporated on top of the thin passivating layers (on both sides). The thin metal layer replicates the surface condition of the passivated contact, whilst remaining sufficiently thin to allow light through, so that the photoconductance (PC) method can be used. PC measurements of the injection-dependent effective carrier lifetime τ_{eff} were taken with a Sinton WCT 120 instrument, using both the transient and quasi-steady-state (QSS) modes. Recombination factors representative of contact region J_{0_cont} were extracted using the Kane and Swanston method, at an injection level ten times that of the base doping, with an intrinsic carrier concentration at 25 °C of $n_i = 8.95 \times 10^9$ cm^{-3}. Passivated recombination factors J_{0_pass} for the two diffusion sets were measured by depositing ~70 nm of plasma-enhanced-chemical-vapour-deposited (PECVD) SiN_x (Roth & Rau AK 400) – a dielectric known to achieve excellent passivation of n⁺ surfaces [11]. The metallised recombination factors J_{0_metal} were obtained by measuring samples with metal directly deposited on the bare silicon surface. These values are included in Table 1.

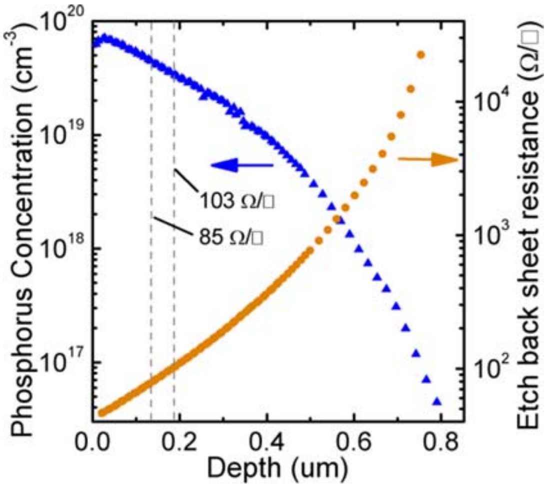

Figure 1 Electrically active phosphorus diffusion profile and associated sheet resistance against diffusion depth. Sheet resistance calculation utilises a model for mobility [10].

Table 1 Characteristics of the etched-back n⁺ diffusion profiles.

R_{sh} (Ω/□)	N_{surf} (cm^{-3})	x_j (µm)	J_{0_metal} (fA cm^{-2})	J_{0_pass} (fA cm^{-2})
85 ± 5	4(±1) × 10^{19}	0.68	1050	55
103 ± 5	3(±1) × 10^{19}	0.61	1250	45

* R_{sh} sheet resistance, N_{surf} surface phosphorus concentration, x_j approximate junction depth, J_{0_metal} recombination factor of metallised n⁺ region, J_{0_pass} recombination factor of passivated n⁺ region.

Transfer length method (TLM) samples, fabricated from identical substrates, were prepared for dielectric film application by the same procedure as the symmetrical lifetime samples described above. Following this, one side of the wafers was coated with passivating dielectrics on top of which 1 µm of aluminium was evaporated. A TLM pattern was defined using photolithography and aluminium etching to achieve pad spacings between 10 µm and 300 µm. Current–voltage measurements were made using a Keithley 2425 Source Meter at 21 ± 3 °C. ρ_c was obtained from an extrapolation of resistance versus pad spacing as described in Ref. [12]. The linear fit used in this extraction consistently produced R^2 statistics of at least 0.99.

Film thickness measurement samples were prepared using single-side mechanically-polished silicon wafers. Due to the dependence of SiO_2 growth on surface dopant concentration, phosphorus diffusion was performed on the SiO_2 thickness samples prior to film growth. Reflectance spectra were obtained using a variable angle ellipsometer (J. A. Woollam M-2000) after growth or deposition of thin passivating films on the polished sides. Indexed optical constants (provided by the device software) for Al_2O_3 and SiO_2 films were used to fit thicknesses.

3 Results and discussion J_{0_cont} and ρ_c as a function of dielectric thickness for the ALD Al_2O_3 series are shown in Fig. 2. These results were obtained by varying the total number of ALD cycles between 1 and 35. Thickness measurements of samples with 15 to 25 cycles revealed an approximately linear growth rate of ~1.0 Å/cycle which was assumed to be the growth rate for all thicknesses.

For dielectric thicknesses between 1 Å and 10 Å, the J_{0_cont} measurements of both the 85 Ω/□ and 103 Ω/□ were seen to decline only slightly, staying roughly equivalent to directly metallised surfaces. The contact resistivity in this region also remained relatively constant. A sharp decrease in J_{0_cont} was observed between 15 Å and 27 Å for both diffusions, following which J_{0_cont} saturated at ~85 fA cm^{-2} – a low value given the ~3 nm thickness of the layer. The fully passivated (i.e. 70 nm PECVD SiN_x, no metal evaporation) recombination factors were found to be only 30–40 fA cm^{-2} lower (see Table 1). As no post-deposition anneal was used before metallisation it is possible that the negative fixed charge, typically associated with ALD Al_2O_3, which may cause increased surface recombination on n$^+$ Si, is absent or weak. This thickness range also results in a dramatic increase in ρ_c by three orders of magnitude, in agreement with previous observations of Loozen et al. [8]. After 25 Å current–voltage measurements revealed non-linear behaviour and the ρ_c could no longer be extracted accurately. A slight lag between the decreasing J_{0_cont} and increasing ρ_c results in an optimum dielectric thickness of ~22 Å. At this thickness a J_{0_cont}/ρ_c combination of 304 fA cm^{-2}/2 mΩ cm^2 is achieved on the 85 Ω/□ diffusion, and 300 fA cm^{-2}/0.3 mΩ cm^2 on the 103 Ω/□ diffusion. A significant improvement in surface passivation following the aluminium metal evaporation was observed; the precise nature of this improvement is not yet understood and is the subject of on-going research.

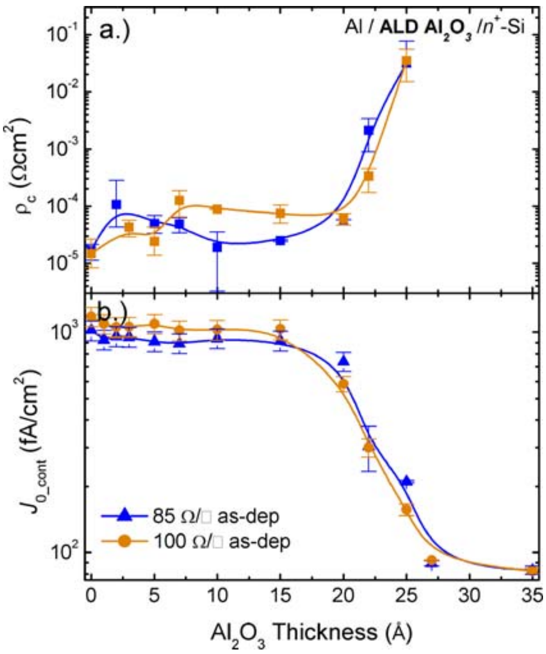

Figure 2 (a) Contact resistivity and (b) contact recombination factor of the ALD Al_2O_3 MIS contacts as a function of the Al_2O_3 thickness. Lines provide a guide to the eyes only. Error bars are based off the measured spread of data and the estimated error of the measurement.

An upper-limit estimate of open-circuit voltage gain ΔV_{oc} (relative to the purely metallised surface) as a result of implementing MIS contacts can be calculated, ignoring other sources of recombination and assuming a 5% contacted fraction, according to

$$\Delta V_{oc} = V_t \ln\left(\frac{0.05 \times J_{0\_metal} + 0.95 \times J_{0\_pass}}{0.05 \times J_{0\_cont} + 0.95 \times J_{0\_pass}}\right), \qquad (1)$$

where V_t represents the thermal voltage. Using this analysis Al_2O_3 MIS contacts could increase the V_{oc} by up to 15 mV.

To investigate the MIS contact thermal stability both TLM and effective lifetime samples were subjected to a 10 minute, 300 °C, forming gas anneal (FGA). This treatment resulted in a large increase in J_{0_cont} to a level just below the fully metallised surface (not shown). This increase could potentially be explained by either aluminium 'spiking' through the ultra-thin Al_2O_3 or the establishment of a substantial negative fixed charge density leading to increased surface recombination. A large decrease in ρ_c was not seen after thermal treatment, suggesting that significant aluminium spiking has not occurred.

Whilst a similar V_{oc} gain is predicted, both the optimum Al_2O_3 thickness and temperature instability of the MIS contacts outlined above are at odds with cell-level results presented by Zielke et al. [2, 3], who found an optimum thickness at 2.4 Å and improved passivation with annealing. These inconsistencies may be partially explained by differences in the ALD oxidising precursor and surface texturing. A longer time interval between HF dip and ALD deposition could also lead to variation in results due to a thicker native oxide (particularly on a n$^+$ surface).

Figure 3 provides the J_{0_cont} and ρ_c trends for the SiO_2 passivated contact with increasing SiO_2 thickness. The SiO_2 layers were grown by dry thermal oxidation at 500 °C for 2.5, 5, 10 or 15 minutes. Polished samples, subjected to the same oxidation conditions with the same phosphorus surface concentration, were measured to have thicknesses in the 14–18 Å range. It is inherent, given the small

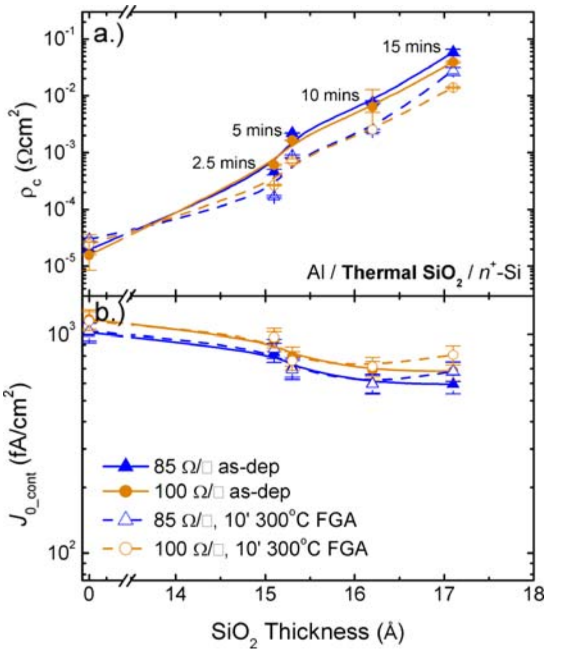

Figure 3 (a) Contact resistivity and (b) Contact recombination factor of the thermal SiO_2 MIS contacts as a function of the SiO_2 thickness. Error bars and lines are based off the same assumptions as in Fig. 2.

thicknesses and short oxidation times, that these extracted thicknesses are subject to a significant uncertainty. Again a decrease in J_{0_cont} is seen with increasing insulator thickness, although not to the same degree – the lowest recombination factors were ~595 fA cm^{-2} for the 85 Ω/□ diffusion and 680 fA cm^{-2} for the 103 Ω/□ diffusion. A corresponding increase in ρ_c is seen in the same thickness range. An estimated optimum combination for high efficiency cells is found at an oxide thickness of ~16 Å (10 minute oxidation). At this thickness a J_{0_cont}/ρ_c combination of 600 fA cm^{-2}/7 mΩ cm^2 is achieved on the 85 Ω/□ diffusion and 685 fA cm^{-2}/6 mΩ cm^2 on the 103 Ω/□ diffusion.

The SiO_2 MIS contact was found to have a greater thermal stability than the Al_2O_3 one. After a 10 minute 300 °C FGA contact resistivity values were more than halved to ~2.5 mΩ cm^2 whilst J_{0_cont} remained relatively constant resulting in upper-limit V_{oc} gains of up to 6 mV. This suggests that the aluminium–SiO_2–silicon MIS contact is compatible with cell fabrication procedures that implement thermal processes (eg. PECVD SiN_x) after contact formation, as aluminium spiking is prevented, in alignment with previously published results [4, 6].

It is worth noting that the Al_2O_3 and SiO_2 passivated contacts demonstrated here could also be applied uniformly to the n^+ rear side of a p^+nn^+ solar cell. In that case, the tolerable contact resistivity for a 100% metal contact fraction is far higher than a partial metal grid. The presented results suggest a total rear J_{0_cont} of ~200 fA cm^{-2} could be achieved using a ~2.5 nm Al_2O_3 layer.

4 Conclusions In this letter we have investigated the contact properties of Al_2O_3 and SiO_2 passivating dielectrics in MIS type contacts on phosphorus diffused regions. In both cases an increasing dielectric thickness leads to a reduction in surface recombination and is accompanied by an increase in contact resistivity. Optimum thicknesses of ALD Al_2O_3 and thermal SiO_2 were found to be ~22 Å and ~16 Å respectively.

The aluminium–Al_2O_3–silicon MIS contacts show an optimum J_{0_pass}/J_{0_cont} combination of 45/300 fA cm^{-2} on a 103 Ω/□ phosphorus diffusion, whilst maintaining a contact resistivity of 0.3 mΩ cm^2. This amounts to a maximum potential V_{oc} gain of 15 mV. These gains are found to diminish significantly after a 300 °C anneal. The aluminium–SiO_2–silicon MIS type contacts exhibit a lower maximum V_{oc} gain of 6 mV but greater thermal stability. An after anneal J_{0_pass}/J_{0_cont} combination of 55/600 fA cm^{-2} with a contact resistivity of 2.5 mΩ cm^2 on a 85 Ω/□ phosphorus diffusion is achieved for this configuration.

Acknowledgements This program has been supported by the Australian Government through the Australian Renewable Energy Agency (ARENA). Responsibility for the views, information or advice expressed herein is not accepted by the Australian Government. Ellipsometer facilities at the Australian National Fabrication Facility were used in this work.

References

[1] R. Woehl et al., IEEE Trans. Electron Devices **58**, 441 (2011).
[2] D. Zielke et al., Phys. Status Solidi RRL **5**, 298 (2011).
[3] D. Zielke et al., Proc. 26th EU PVSEC, 2011, p. 1115.
[4] J. Schmidt et al., Progr. Photovolt. **16**, 461 (2008).
[5] M. Green et al., Proc. 15th IEEE PVSEC, 1981, p. 1405.
[6] K. Jäger-Hezel et al., Proc. 13th EU PVSEC, 1995, p. 1515.
[7] A. Metz et al., Proc. 26th IEEE PVSEC, 1997, p. 283.
[8] X. Loozen et al., Energy Procedia **21**, 75 (2012).
[9] J. Nekarda et al., Proc. 34th IEEE PVSEC, 2009, p. 892.
[10] D. B. M. Klaassen, Solid-State Electron. **35**, 953 (1992).
[11] M. Kerr et al., J. Appl. Phys. **89**, 3821 (2001).
[12] D. K. Schroder, Semiconductor Material and Device Characterisation (Wiley, Hoboken, 2006), p. 146.